LUNAR SURFACE CHARGING: A GLOBAL PERSPECTIVE USING LUNAR PROSPECTOR DATA.

T. J. Stubbs[1], J. S. Halekas[2], W. M. Farrell[1], and R. R. Vondrak[1], [1]NASA Goddard Space Flight Center, Greenbelt, MD 20771, USA, [2]University of California, Berkeley, CA 94720, USA. Timothy.J.Stubbs.1@gsfc.nasa.gov.

Introduction: Our aim here is to use moments of the electron distribution function derived from Lunar Prospector Electron Reflectometer (LP/ER) data [1], together with basic probe equations [2], to determine the global variation in lunar surface electrostatic potentials for the different plasma environments encountered by the Moon. This will be a first step in better understanding and predicting global lunar surface charging under various conditions. This work will also include some simple estimates of the horizontal electric fields near the lunar terminator.

The surface of the Moon, like any object in a plasma, charges to an electrostatic potential that minimizes the total incident current [3]. The charging currents come from four sources: photoemission of electrons (J_{ph}), plasma electrons (J_e), plasma ions (J_i), and secondary electrons (J_{sec}). (J_{sec} arises primarily from surface ionization by plasma electrons.) The Moon is exposed to a variety of plasma environments during its orbit such that incident currents span several orders of magnitude. For about three-quarters of the time, the Moon is in the solar wind flow; otherwise, it is either in the tenuous plasma of the magnetospheric tail lobes, or the turbulent and energetic plasmas encountered in the geomagnetic plasma sheet and magnetosheath.

The lunar dayside typically charges positive, since J_{ph} usually dominates (see Fig. 1). As a result a "photoelectron sheath" forms above the surface, which in the solar wind extends ~1m, and effectively shields the charged surface from the surrounding plasma [4]. On the nightside, the lunar surface usually charges negative since J_e typically dominates. In this case a "Debye sheath" shields the surface potential [5] and can extend from meters to possibly ~1km [6]. There are significant uncertainties in current estimates of lunar surface potentials and almost nothing is known about their spatial distribution and temporal variation.

Implications: Surface charging processes are thought to drive the transport of lunar dust grains with radii <10μm, particularly near the terminator. The Surveyor landers observed ≈5μm grains levitating ~10cm above the surface [7,8]. During the Apollo missions 0.1μm-scale dust in the lunar exosphere was observed up to ~100km altitude [9,10,11]. The most viable mechanisms proposed to explain these observations have been based on the principle that the like-charged surface and dust grains act to repel each other such that dust is ejected from the surface. Under certain conditions, the heavier grains are predicted to electrostatically levitate near the surface [5,12], while the smaller grains are electrostically "lofted" to ~10km in altitude [13,14]. These phenomena could present a significant hazard to future robotic and human exploration of the Moon [15,16].

Spacecraft and Instrumentation: The LP spacecraft was in a rapidly precessing polar orbit about the Moon (period ~2 hours), which gave full coverage of the lunar surface twice every lunation. LP collected data for 18 months, with its altitude varying between 20 and 115 km, thus providing good coverage under most conditions. ER data is used to calculate electron concentrations (n_e) and temperatures (T_e) from kappa fits to the electron distribution functions [1]. As there is no ion data from LP we assume that the plasma near the Moon is quasi-neutral and the electrons and ions have the same temperature, i.e., $n_i = n_e$ and $T_i = T_e$.

Surface Charging Model: We calculate the electrostatic surface potential, ϕ_S, using the method and equations given in [2]. We solve numerically to find ϕ_S such that the net incident current is approximately zero, i.e., $J_e + J_i + J_{ph} \approx 0$. ($J_{sec}$ is not included here since on the dayside and near the terminator it is expected to be

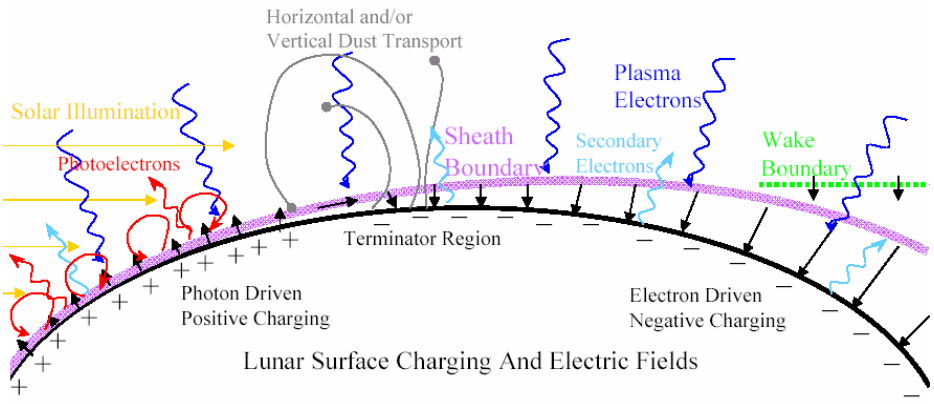

Fig. 1. Schematic of lunar electrostatic environment, showing charging current sources, surface charge, and electric fields (not to scale).

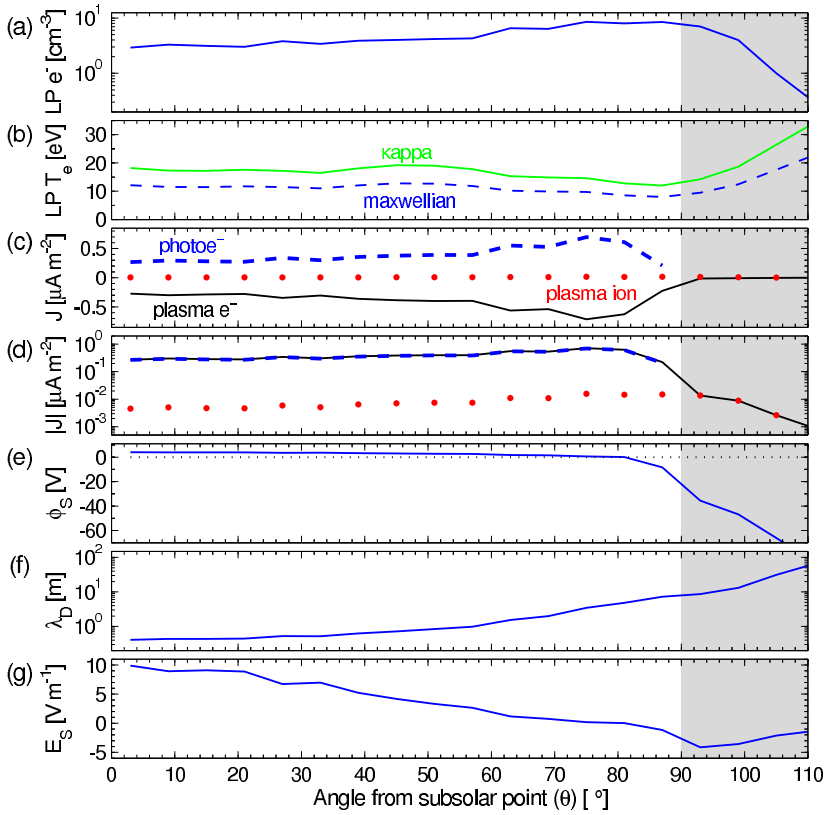

Fig. 2. Lunar surface charging predictions under typical solar wind conditions plotted as a function of angle from the subsolar point (θ). Input data: LP/ER derived electron (a) concentrations and (b) kappa (solid line) and maxwellian (broken line) temperatures. Current contributions from J_e (broken line), J_i (dots) and J_{ph} (solid line) shown on (c) linear and (d) log scales. (e) Lunar surface potential, ϕ_S, (f) Debye length of attracted species, λ_D, and (g) Surface electric field, E_S.

less significant than either J_e, J_i or J_{ph}.) The current density equations are different for positive ($\phi_S > 0$) and negative ($\phi_S < 0$) surface potentials [14]. Photocurrent density from normally incident sunlight is assumed to be 4.0×10^{-6} A m^{-2} [17] (given a surface photoelectron efficiency of 0.1). J_{ph} varies with the angle from the subsolar point, θ, and so is highest at the equator at local noon ($\theta = 0°$) and drops off to zero at the terminator ($\theta = 90°$). The Debye lengths used in this model are for the species attracted to the surface (e.g., where $\phi_S > 0$ we use the electron Debye length). It is important to note that the dominant source of electrons on the lunar dayside is from photoemission (at ~500 cm^{-3} this is ~100 times greater than in the solar wind). Assuming 1-D Debye shielding above a plane, the lunar surface electric field is given by $E_S = \phi_S / \lambda_D$.

Initial Predictions: Fig. 2 shows predictions for lunar surface charging given typical solar wind conditions. As expected the dayside is photo-driven ($\phi_S > 0$) and the nightside is electron-driven ($\phi_S < 0$). Due to the lower plasma concentrations, the nightside currents are much weaker.

In Fig. 2 we have only considered the vertical component of E_S. Horizontal electric fields will form between regions of different potential, and we would expect this to be most significant near the transition from $\phi_S > 0$ to $\phi_S < 0$ (i.e., near the terminator). We will make zeroth order estimates of horizontal E_S using a similar method to that described above. This could explain the enhancement in horizontal dust transport observed in-situ by the Apollo 17 LEAM experiment near the terminators [18,19].

References: [1] Halekas, J.S., et al. (2002) Geophys. Res. Lett., 2001GL014428. [2] Manka, R.H. (1973) Photon & Particle Interactions with Surfaces in Space, 347. [3] Whipple, E.C. (1977) J. Geophys. Res., 1525. [4] Singer, S.F. and Walker, E.H. (1962) Icarus, 1, 7. [5] Nitter, T. et al. (1998) J. Geophys. Res., 6605. [6] Halekas, J.S., et al. (2003) Geophys. Res. Lett., 2003GL018421. [7] Criswell, D.R. (1973) Photon & Particle Interactions with Surfaces in Space, 545. [8] Rennilson, J.J. and Criswell, D.R. (1974) The Moon, 10, 121. [9] McCoy, J.E. and Criswell, D.R. (1974) Proc. Lunar Sci. Conf. 5th, 2991. [10] McCoy, J.E. (1976) Proc. Lunar Sci. Conf. 7th, 1087. [11] Zook, H.A. and McCoy, J.E. (1991) Geophys. Res. Lett., 18, 2117. [12] Sickafoose, A.A. et al. (2002) J. Geophys. Res. 2002JA009347. [13] Stubbs, T.J., et al. (2005) Adv. Space Res., in press. [14] Stubbs, T.J., et al. (2005) Lunar Planet. Sci. Conf. 36th, 1899. [15] NASA Robotic and Human Lunar Exploration Strategic Roadmap (2005). [16] Stubbs, T.J., et al. (2005) Lunar Planet. Sci. Conf. 36th, 2277. [17] Goertz, C.K. (1989) Rev. Geophys., 27, 271. [18] Berg, O.E., et al. (1976) Interplanetary Dust and Zodiacal Light, 233. [19] Berg, O.E. (1978) Earth Planet. Sci. Lett., 39, 377.